

Supplementary Information

Construction of "peptide-hemin/DNA" hybrid-complexes and their peroxidase activities

Jing Liu,^{‡a} Taozhe Zhang,^{‡a} Jinyang Feng,^a Yue Cui,^a Li Zhang,^a Yunong Wang,^a Meiyu Cui,^a
Donghao Li^{*,a} and Hulin Tai^{*,a,b,c}

^aInterdisciplinary Program of Biological Functional Molecules (College of Integration Science), Department of Chemistry (College of Science), Yanbian University, Yanji 133002, China; ^bNational Demonstration Centre for Experimental Chemistry Education, Yanbian University, Yanji 133002, Jilin, China; ^cJilin Key Laboratory for Immune and Targeting Research on Common Allergic Diseases, Yanbian University, Yanji 133002, Jilin, China

*E-mail: taihulin@ybu.edu.cn, dhli@ybu.edu.cn; Phone: +86-433-273-3736

[‡] These authors are contributed equally to this work.

Contents

Experimental Section, References, and Author Contributions	p. S2
Fig. S1 Schematic representation of various G4s	p. S4
Fig. S2 Mass spectra of MP11 and AcMP11	p. S5
Fig. S3 pH-dependent ¹ H NMR spectra of the AcMP11–[d(TTAGGG)] ₄ hybrid-complex	p. S6
Fig. S4 ¹ H NMR spectra of the AcMP11–[d(TTAGGG)] ₄ hybrid-complex in 90% ¹ H ₂ O/10% ² H ₂ O and 2% ¹ H ₂ O/98% ² H ₂ O	p. S7
Table S1 DNA base proton shifts (ppm) of the free and complex	p. S8
Fig. S5 ¹ H- ¹ H NOESY spectrum of the AcMP11–[d(TTAGGG)] ₄ hybrid-complex	p. S9
Fig. S6 ¹ H- ¹ H TOCSY spectrum of the AcMP11–[d(TTAGGG)] ₄ hybrid-complex	p. S10
Fig. S7 Absorption spectra of AcMP11 and AcMP11–[d(TTAGGG)] ₄ hybrid-complex	p. S11
Fig. S8 Absorption spectra of hemin in the presence of various stoichiometric ratios of [d(TTAGGG)] ₄	p. S12
Fig. S9 Absorption spectra of AcMP11 in the presence of various stoichiometric ratios of parallel G-quadruplex DNAs	p. S13
Fig. S10 Time-evolution of 414 nm absorbance due to ABTS oxidation by the hybrid-complexes in the presence of [H ₂ O ₂] = 4mM	p. S14
Fig. S11 Time-evolution of 414 nm absorbance due to ABTS oxidation by the hybrid-complexes in the presence of various H ₂ O ₂ concentration	p. S15

Experimental Section

Sample Preparation.

Microperoxidase-11 (MP11, Sigma Aldrich) was dissolved by 200 mM sodium carbonate buffer (pH10.0) while 500 molar equivalents of acetic anhydride were slowly added to acetylate the α -NH₂ group of Valine11 and the ϵ -NH₂ group of Lysine13.¹ Potassium hydroxide was added as needed to maintain a solution pH of 9 – 10. The reaction mixture was stirred in an ice water bath for 3 hours. Acetylated MP11 (AcMP11) was exchanged into ultrapure water using an Amicon Stirred Cell concentrator (molecular weight cutoff, 1 kDa) and lyophilized by a vacuum freeze dryer (FDU-1200, EYELA, Japan). The concentration of AcMP11 was determined spectrophotometrically using the absorbance at 397 nm (molar extinction coefficient $\epsilon_{397} = 147167 \text{ cm}^{-1} \text{ M}^{-1}$).²

d(TTAGGG), d(TTAGGGp), d(TTAGGGT) and d(TAGGGTGGGTTGGGTGIG) purified with a HPLC cartridge was purchased from Sangon Biotech (Shanghai) Co., Ltd. The oligonucleotide was obtained by ethanol precipitation, and then desalted with a size exclusion column (Tskgel G3000PW, TOSOH, Japan). The concentration of each oligonucleotide was determined spectrophotometrically using the absorbance at 260 nm ($\epsilon_{260} = 6.89 \times 10^4$, 6.89×10^4 , 7.81×10^4 and $2.01 \times 10^5 \text{ cm}^{-1} \text{ M}^{-1}$ for the d(TTAGGG), d(TTAGGGp), d(TTAGGGT) and d(TAGGGTGGGTTGGGTGIG), respectively).³ G-quadruplex DNAs (G4s) were forming through annealing of oligo-nucleotides in the presence 300 mM KCl and 50 mM potassium phosphate buffer, pH6.80.⁴ The samples were annealed by heating at 95°C for 5 min and then slowly cooling to room temperature overnight. For 2D NMR sample preparation of the AcMP11–[d(TTAGGG)]₄ hybrid-complex, 125 μL of 4 mM AcMP11 solution was lyophilized by the freeze dryer, and dissolved by 250 μL of 2.2 mM [d(TTAGGG)]₄ solution in 300 mM KCl and 50 mM potassium phosphate buffer, pH6.80. Thus, the final concentrations of the AcMP11 and [d(TTAGGG)]₄ in the solution mixture were 2 and 2.2 mM, respectively. The ²H₂O content of the samples was either ~10% or ~98%. The pH of the resulting solution was adjusted using 0.2 M KOH or 0.2 M HCl, if necessary. The pH value was monitored by an F-73G pH meter with a 9618S-10D electrode (Horiba, Japan).

Mass Measurements.

The molecular weight of the MP11 and AcMP11 were measured with a 2D μ CFs-TOF-HRMS Impact II (Bruker).⁵ The experimental settings for the mass spectrometry were optimized automatically. The results were processed using the Bruker Compass Data Analysis version 4.3.110.102 with the instrument. The MP11 and AcMP11 samples were adjusted by ultrapure water to the concentrations of ~15 and ~150 μM , respectively. The injection volume and the flow rate were 5 μL and 300 $\mu\text{L}/\text{min}$, respectively. Full mass spectra were acquired in the positive ionization mode over the m/z 50 – 2000 range.

NMR Measurements.

¹H NMR spectra were recorded on Bruker AVANCE III Ascend 500HD spectrometer operating at ¹H frequency of 500 MHz. One-dimensional ¹H NMR spectra of the AcMP11 and AcMP11–G4s hybrid-complexes were obtained with a 199.9 ppm spectral width, 32k data points, a 1.5 s relaxation delay, and 512 transients. Water suppression was achieved by the presaturation method. The signal-to-noise ratio of the spectra was improved by apodization, which introduced 10 Hz line-broadening. The NMR spectra were processed using Bruker TopSpin version 3.6.3 (Bruker BioSpin).

Two-dimensional nuclear Overhauser effect spectroscopy (NOESY) and total correlation spectroscopy (TOCSY) spectra of the AcMP11–G4 hybrid-complex were acquired by quadrature detection in the phase-sensitive mode with a States-TPPI,⁶ with a 15 ppm spectral width, 8k \times 512 data points, a 1.5 s relaxation delay, at 25 °C. The NOESY and TOCSY spectra were recorded using mixing times of 100 and 80 ms, respectively. A phase-shifted sine-squared window function was

applied to both dimensions before two-dimensional Fourier transformation. The chemical shifts for ^1H NMR spectra are referred to external 2,2-dimethyl-2-silapentane-5-sulfonate.

Absorption Measurements.

UV-Vis absorption spectra were recorded at 298 K with UV-2700 and UV-3600Plus spectrophotometers (SHIMAZU, Japan). In order to characterize the complexations between AcMP11 and G4s, 2 – 5 μM AcMP11 in 300 mM KCl and 50 mM potassium phosphate buffer (pH6.80) were titrated against the G4s at 25 $^\circ\text{C}$.

Kinetic studies were performed on the UV-2700 spectrometer. A chromogenic substrate, 2,2'-Azinobis-(3-ethylbenzthiazoline-6-sulphonate) (ABTS), was purchased from Sigma-Aldrich, and the peroxidase reaction was monitored by following the appearance of the oxidized product, ABTS^{++} through the following reaction, which absorbance at ~ 414 nm. Sample of the AcMP11–[d(TTAGGGT)]₄ hybrid-complex comprised 0.1 μM AcMP11, 352.4 μM [d(TTAGGGT)]₄, and 0.5 mM ABTS. Sample of the AcMP11–[d(TTAGGGp)]₄ hybrid-complex comprised 0.1 μM AcMP11, 32.4 μM [d(TTAGGGp)]₄, and 0.5 mM ABTS. Sample of the AcMP11–NG18I hybrid-complex comprised 0.1 μM AcMP11, 9.3 μM NG18I, and 0.5 mM ABTS. Sample of the AcMP11–[d(TTAGGG)]₄ hybrid-complex comprised 0.1 μM AcMP11, 2.4 μM [d(TTAGGG)]₄, and 0.5 mM ABTS. The percentages of formation of the hybrid-complexes are more than 98% based on the K_a values. To initiate the oxidation reaction, 0 – 8 mM hydrogen peroxide (H_2O_2) was added to the solution mixture. The initial slope (R_0) of the time evolution of 414-nm absorbance due to ABTS^{++} was used as an index for the peroxidase activity.

Author Contributions

H.T. and D.L. conceived and designed the project. J.L., T.Z., and H.T. performed the sample preparations. H.T. and J.L. performed the NMR measurements. J.L., T.Z., J.F., Y.C., L.Z., N.W., and H.T. performed the absorption measurements. J.L., T.Z., and C.M. performed the mass measurements. H.T., J.L., and T.Z. analyzed the spectroscopic data. H.T. wrote the manuscript with contributions from all the other authors.

References

1. (a) O. Q. Munro and H. M. Marques, *Inorg. Chem.*, 1996, **35**, 3752-3767; (b) H. M. Marques and C. B. Perry, *J. Inorg. Biochem.*, 1999, **75**, 281-291.
2. N. J. O'Reilly and E. Magner, *Phys. Chem. Chem. Phys.*, 2011, **13**, 5304-5313.
3. H. Araki, S. Hagiwara, R. Shinomiya, A. Momotake, H. Kotani, T. Kojima, T. Ochiai, N. Shimada, A. Maruyama and Y. Yamamoto, *Biomater. Sci.*, 2021, **9**, 6142-6152.
4. (a) K. Saito, H. Tai, M. Fukaya, T. Shibata, R. Nishimura, S. Neya and Y. Yamamoto, *J. Biol. Inorg. Chem.*, 2012, **17**, 437-445; (b) K. Saito, H. Tai, H. Hemmi, N. Kobayashi and Y. Yamamoto, *Inorg. Chem.*, 2012, **51**, 8168-8176.
5. Z. Wang, H. B. Shang, M. Cui, B. Ma, D. Li, D. Jin and M. Dong, *J. Chromatogr. A*, 2022, **1685**, 463641.
6. D. J. States, R. A. Haeberkorn and D. J. Ruben, *J. Magn. Reson.*, 1982, **72**, 286-292.
7. (a) Y. Wang and D. J. Patel, *Biochemistry*, 1992, **31**, 8112-8119; (b) V. Kuryavyi, L. A. Cahoon, H. S. Seifert and D. J. Patel, *Structure*, 2012, **20**, 2090-2102.
8. (a) H. Tai, S. Nagatomo, H. Mita, Y. Sambongi and Y. Yamamoto, *Bull. Chem. Soc. Jpn.*, 2005, **78**, 2019-2025; (b) H. M. Marques, *Dalton Trans.*, 2007, **36**, 4371-4385.
9. T. Ohyama, Y. Kato, H. Mita and Y. Yamamoto, *Chem. Lett.*, 2006, **35**, 126-127.

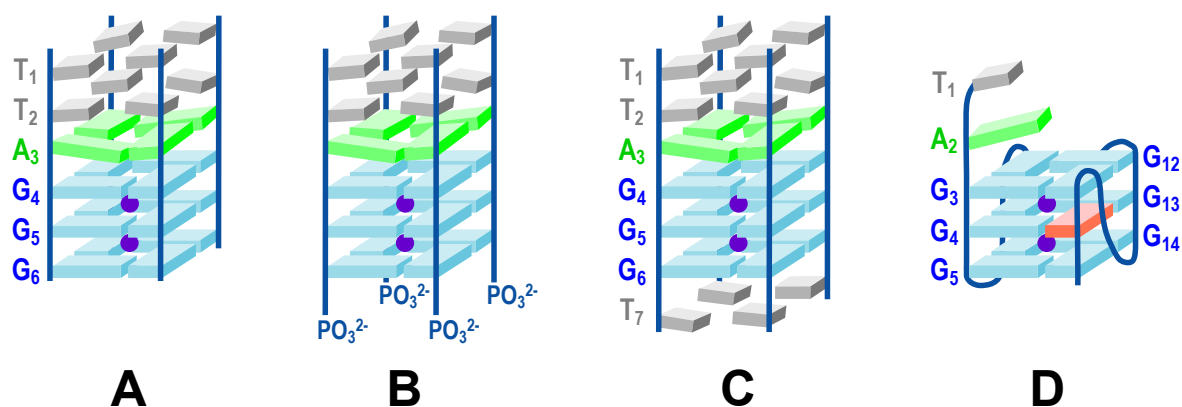


Fig. S1 Schematic representation of parallel G-quadruplex DNAs formed from d(TTAGGG), d(TTAGGGp), d(TTAGGGT), and non-standard base inosine(I)-containing sequence d(TAGGGTGGGTTGGGTGIG), i.e., [d(TTAGGG)]₄ (A), [d(TTAGGGp)]₄ (B), [d(TTAGGGT)]₄ (C) and (NG18I) (D), respectively.^{3,7} The inosine base represented a red colour in the NG18I.

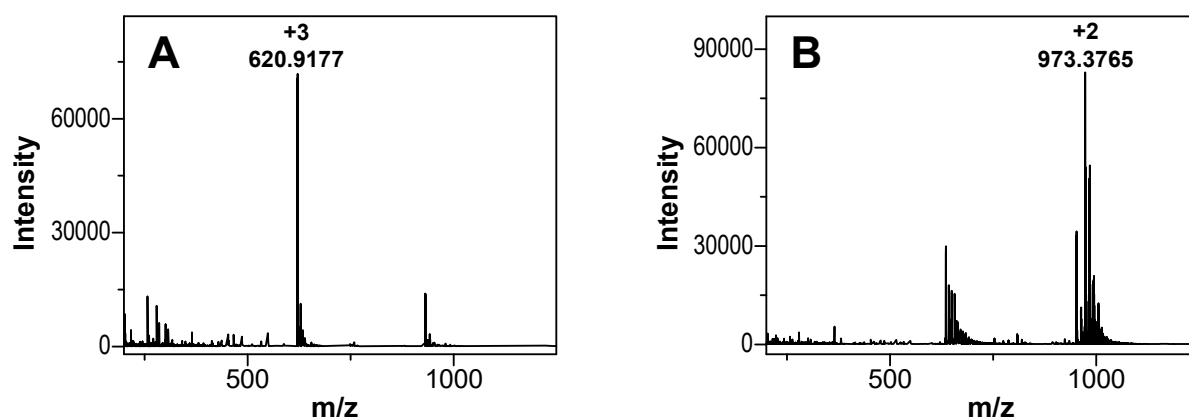


Fig. S2 Mass spectra of MP11 (A) and AcMP11 (B). The concentrations of MP11 and AcMP11 samples are ~ 15 and ~ 150 μM , respectively. In the case of MP11, one major ion was observed at m/z 620.9177, which indicated $z = 3$. Whereas, in the case of AcMP11, one major ion was observed at m/z 973.3765, which indicated $z = 2$. The theoretical molecular weight (MW) values of MP11 and AcMP11 are 1861.94 and 1946.01, respectively. The experimentally observed MW values are in good agreement with the theoretical values.

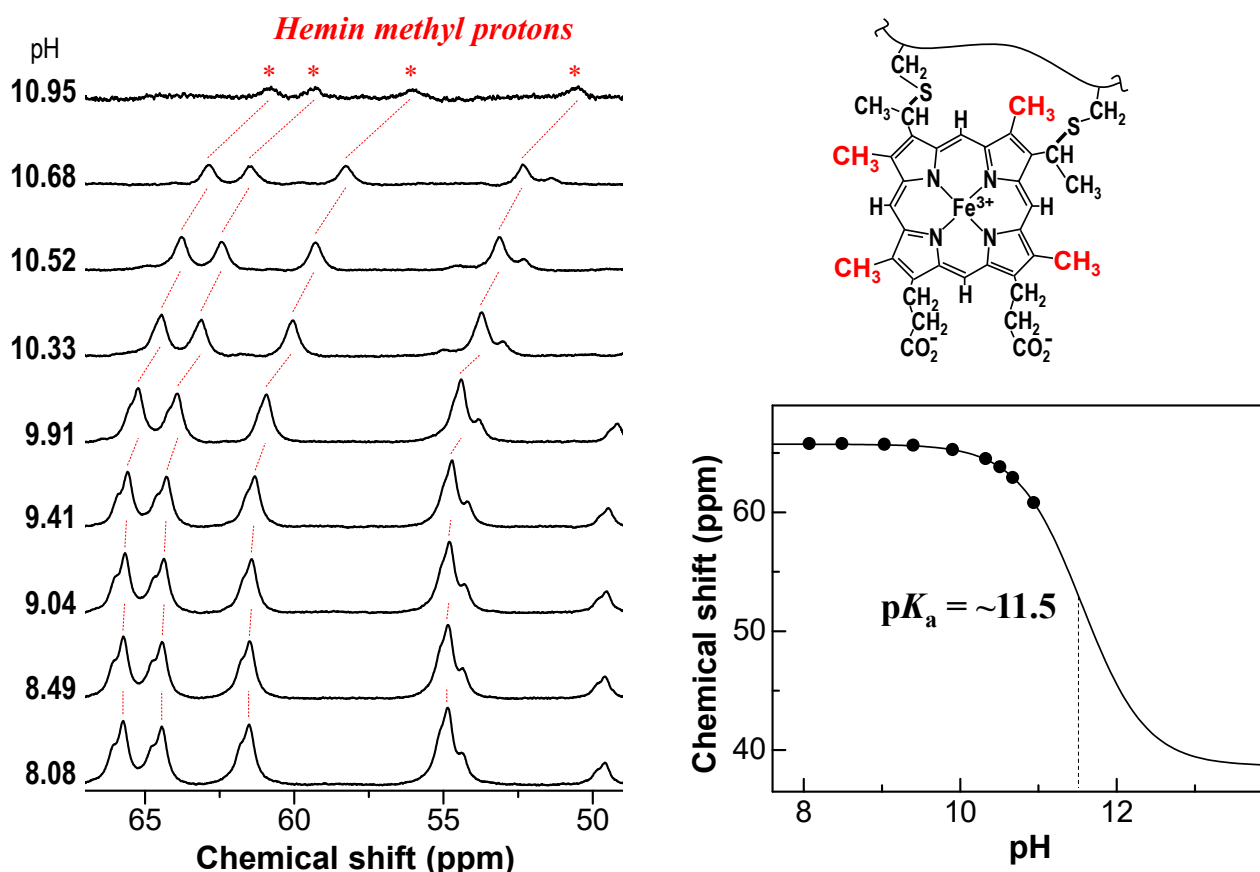


Fig. S3 Down-shifted portions of the ^1H NMR spectra of the AcMP11-[d(TTAGGG)]₄ hybrid-complex in 90% $^1\text{H}_2\text{O}$ /10% $^2\text{H}_2\text{O}$, 300 mM KCl, 50 mM potassium phosphate buffer at 25 °C and the indicated pHs (left). The plot of the observed shifts of the hemin methyl proton signal against the pHs (right). The hemin methyl proton signals in the spectra of each hybrid-complex are connected by dotted lines. The molecular structure of the c-type heme is schematically illustrated in the upper right corner. A pK_a value was observed at ~ 11.5 .

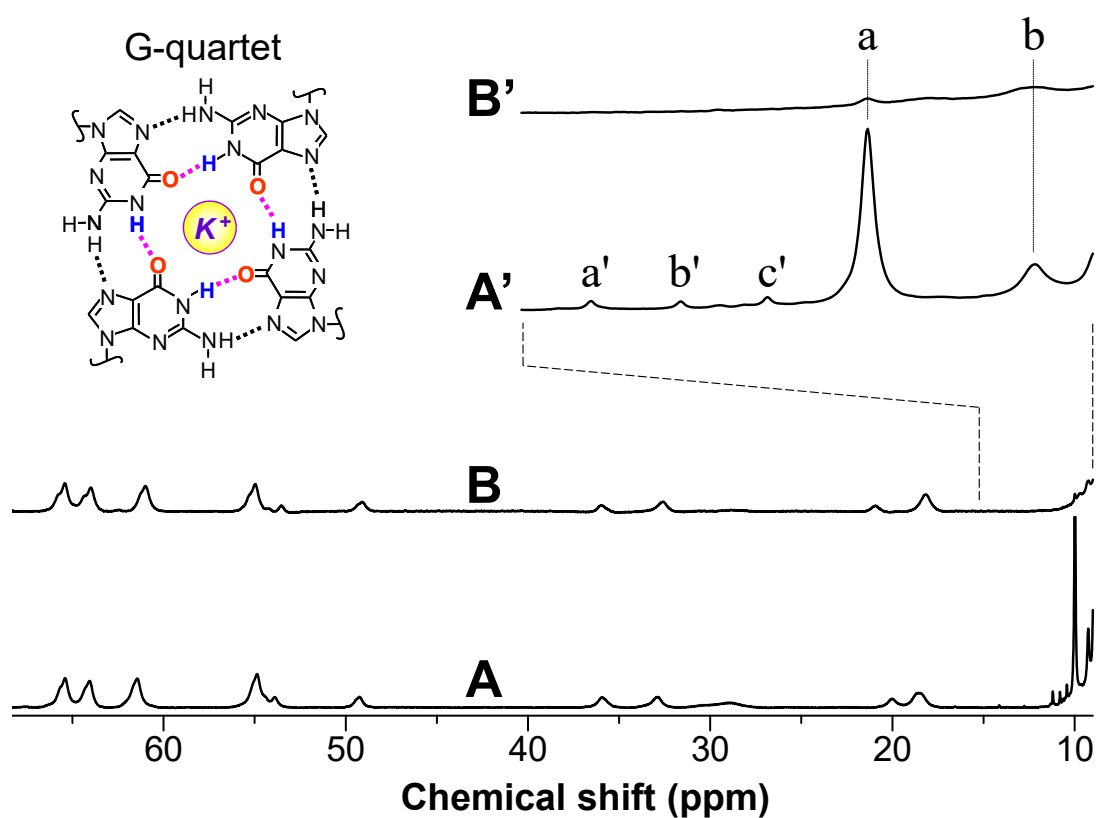


Fig. S4 ^1H NMR spectra of the AcMP11–[d(TTAGGG)]₄ hybrid-complex in 90% $^1\text{H}_2\text{O}$ /10% $^2\text{H}_2\text{O}$ (A and A') and 2% $^1\text{H}_2\text{O}$ /98% $^2\text{H}_2\text{O}$ (B and B'), with 300 mM KCl and 50 mM potassium phosphate buffer at pH6.80 and 25 °C. The molecular structure of the G-quartet is schematically illustrated in the upper left corner. Peaks a' – c' and a – b are due to guanine imino protons of the free and AcMP11-bound [d(TTAGGG)]₄, respectively.

Table S1 The DNA base protons shifts (ppm) of [d(TTAGGG)]₄ and AcMP11–[d(TTAGGG)]₄ complex in 90% H₂O/10% ²H₂O, 300 mM KCl, 50 mM potassium phosphate buffer, pH6.80, and 25 °C

	NH			H2/H8	H6	
	G ₆	G ₅	G ₄	A ₃	T ₂	T ₁
Free	10.42	10.80	11.20	8.00/8.28	7.20	7.30
Complex	n.d. ^b	9.26	9.99	7.75/8.08	7.06	7.20
$\Delta\delta^a$	n.d. ^b	–1.54	–1.21	–0.25/–0.20	–0.14	–0.10

a) The differences in the shift between the corresponding signals of AcMP11–[d(TTAGGG)]₄ complex and [d(TTAGGG)]₄, i.e., $\Delta\delta = \delta_{\text{complex}} - \delta_{\text{G4}}$. b) Not determined due to extremely large line broadening.

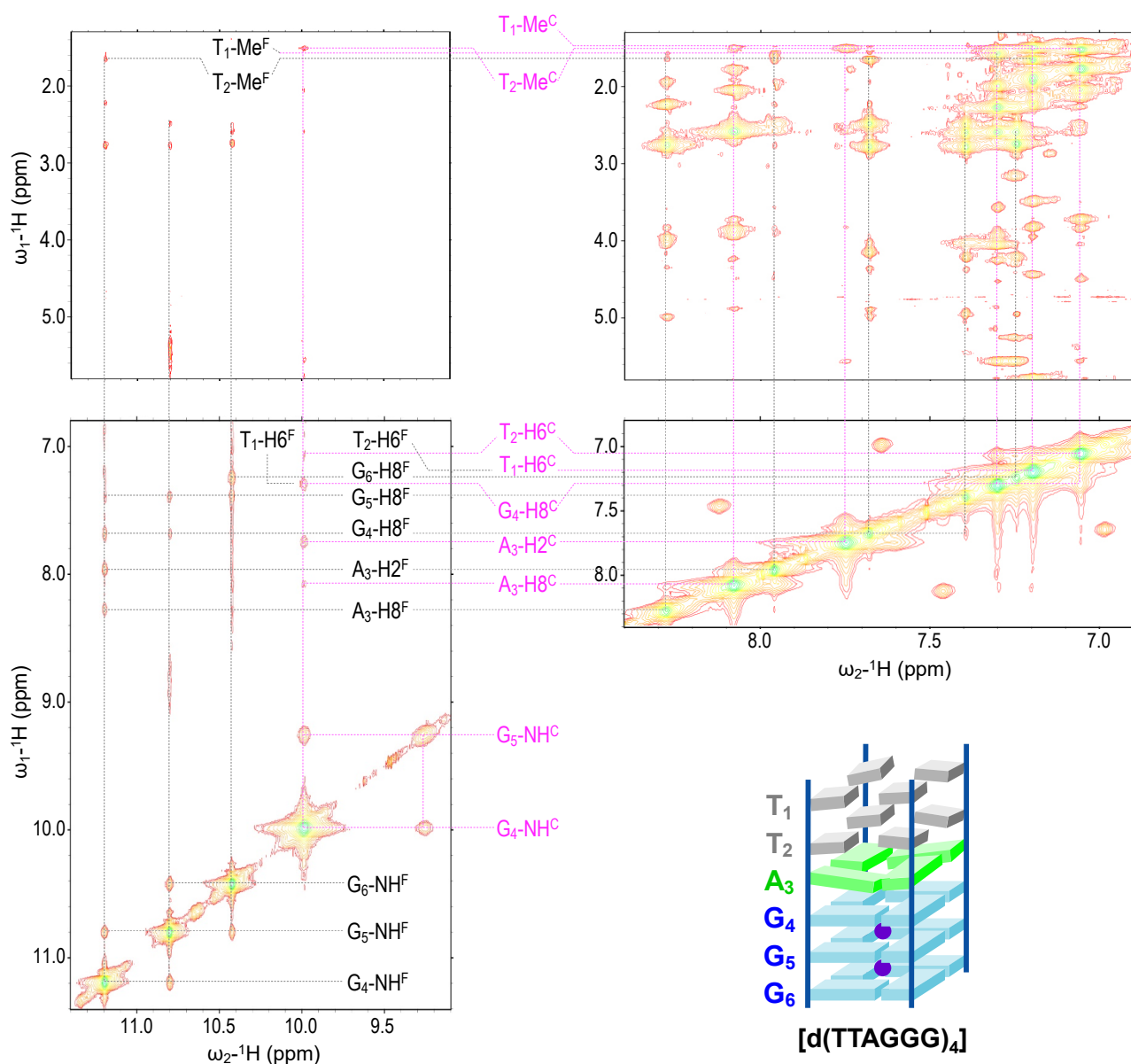


Fig. S6 Portions of the ^1H - ^1H NOESY spectrum of $[\text{d}(\text{TTAGGG})]_4$ in the present of 0.9 equivalent of AcMP11 in 90% $^1\text{H}_2\text{O}$ /10% $^2\text{H}_2\text{O}$, 300 mM KCl and 50 mM potassium phosphate buffer at pH 6.80 and 25 °C. Schematic representation of structure of the $[\text{d}(\text{TTAGGG})]_4$ is illustrated in the under right corner. A mixing time of 100 ms was used to record the NOESY spectrum. Signal assignments of the selected proton signals are shown with the spectra. For example, $\text{G}_n\text{-NH}^{\text{F}}$ and $\text{G}_n\text{-NH}^{\text{C}}$, where $n = 4, 5$, or 6 , represent the free $[\text{d}(\text{TTAGGG})]_4$ and AcMP11- $[\text{d}(\text{TTAGGG})]_4$ complex, respectively.

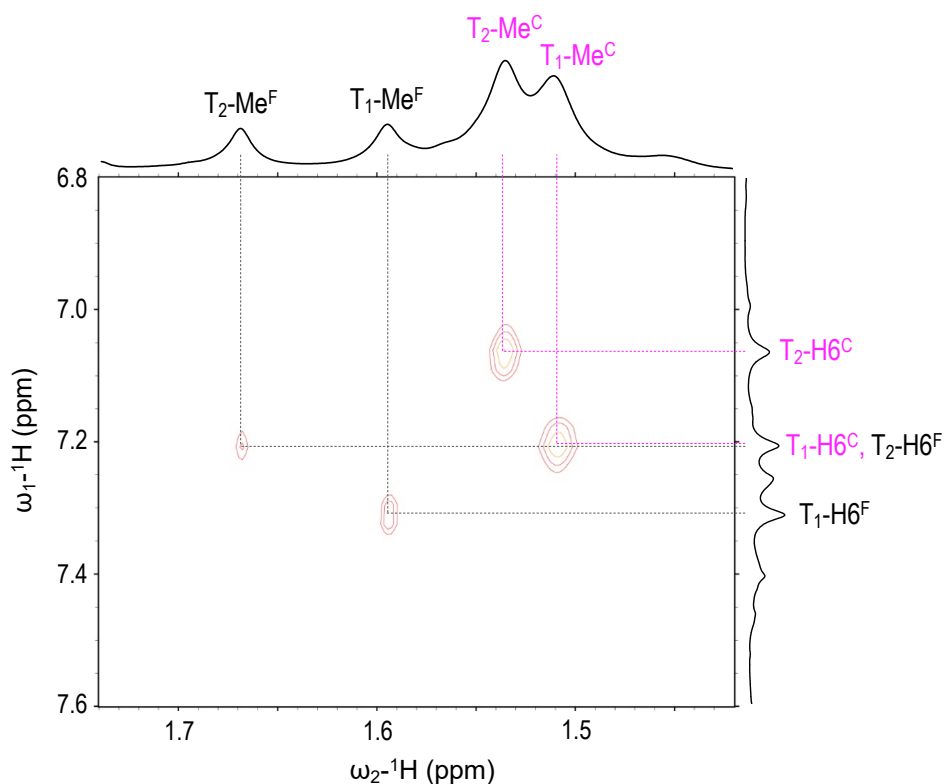


Fig. S7 Portions of the ^1H - ^1H TOCSY spectrum of $[\text{d}(\text{TTAGGG})]_4$ in the present of 0.9 equivalent of AcMP11 in 90% $^1\text{H}_2\text{O}$ /10% $^2\text{H}_2\text{O}$, 300 mM KCl and 50 mM potassium phosphate buffer at pH6.80 and 25 °C. A mixing time of 80 ms was used to record the spectrum. Signal assignments of the selected protons of T_1 -Me, T_1 -H6, T_2 -Me and T_2 -H6 are shown with the spectra. For example, $\text{T}_n\text{-H6}^{\text{F}}$ and $\text{T}_n\text{-H6}^{\text{C}}$, were $n = 1$ or 2 , represent the free $[\text{d}(\text{TTAGGG})]_4$ and AcMP11- $[\text{d}(\text{TTAGGG})]_4$ complex, respectively.

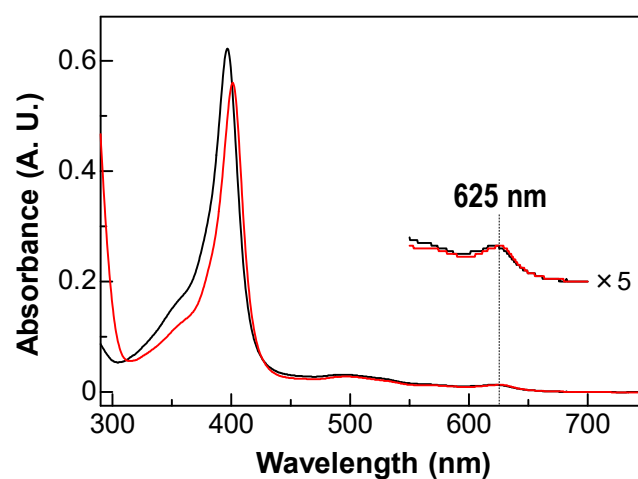


Fig. S8 Absorption spectra of AcMP11 (black) and AcMP11-[d(TTAGGG)]₄ hybrid-complex (red) in 300 mM KCl and 50 mM potassium phosphate buffer at pH6.80 and 25 °C. Magnified spectrum (×5) in the 550 – 700 nm region is also shown. The absorbance at ~625 nm is characteristic of a ferric high-spin ($S = 5/2$) hemin.⁸

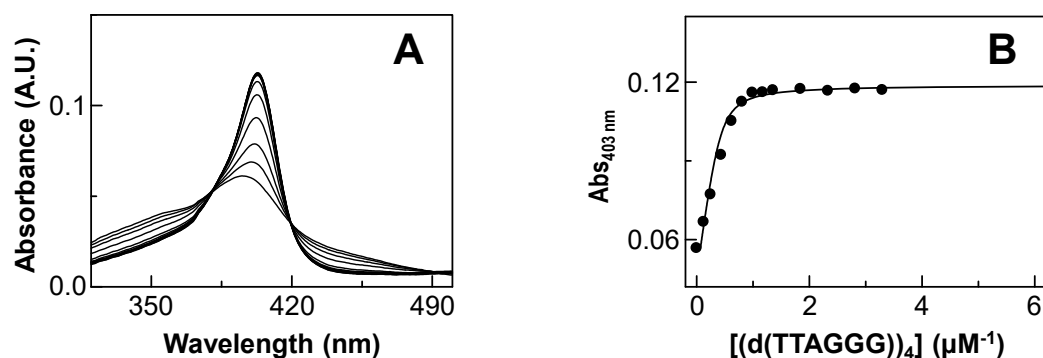


Fig. S9 (A) Absorption spectra, 320 – 500 nm, of hemin in the presence of various concentrations of [d(TTAGGG)]₄, in 300 mM KCl and 50 mM potassium phosphate buffer, pH6.80, together with 0.08 w/v% Triton X-100 and 0.5 v/v% DMSO, at 25 °C. (B) Plot of the 403 nm absorbance against concentration of [d(TTAGGG)]₄. A hemin binding constant (K_a) value of $21.46 \pm 1.85 \mu\text{M}^{-1}$ was obtained for the hemin–[d(TTAGGG)]₄ complex. The K_a value was in agreement with that reported previously for the hemin–[d(TTAGGG)]₄ complex.⁹

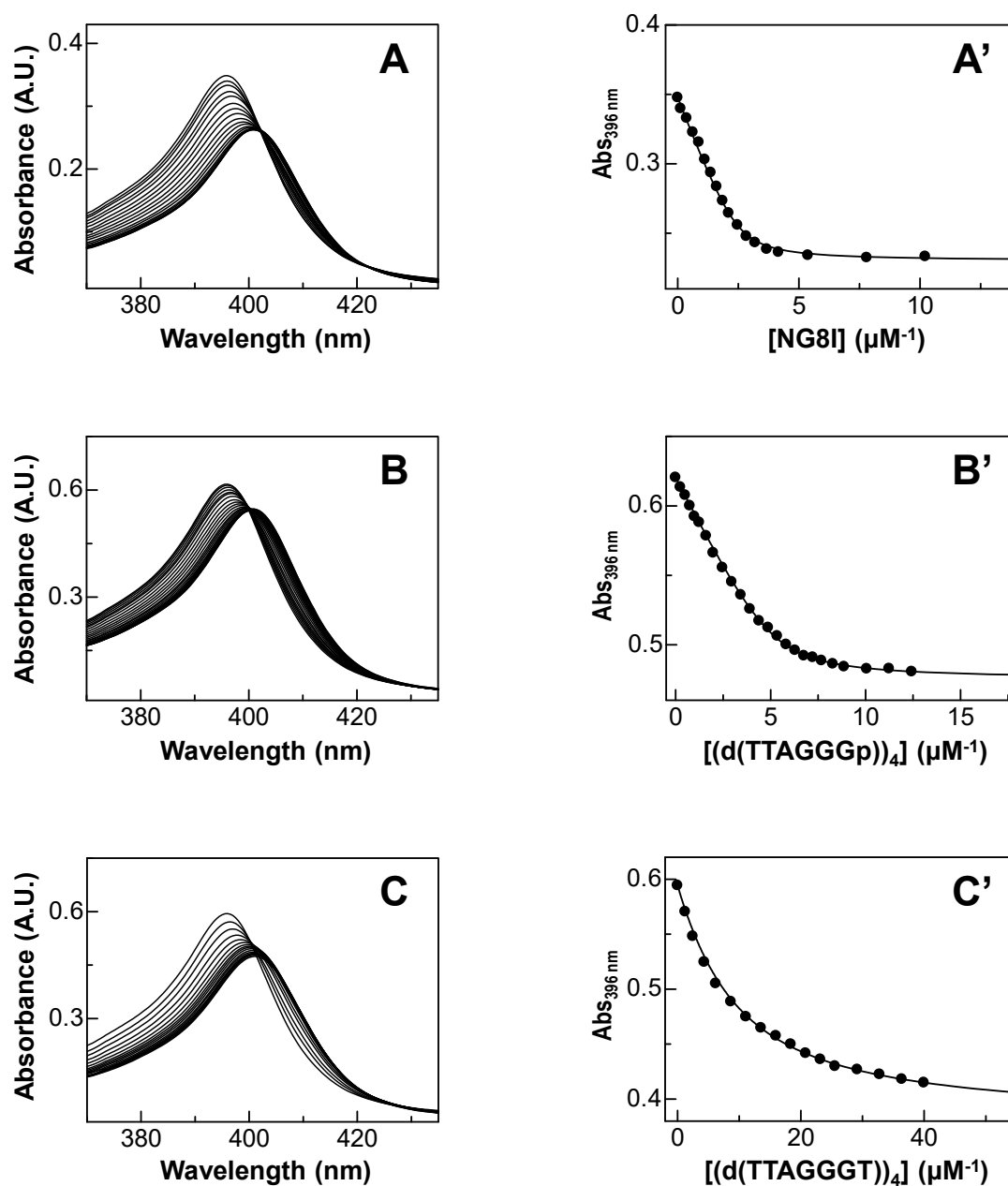


Fig. S10 Absorption spectra, 370 – 435 nm, of AcMP11 in the presence of various concentrations of NG8I (A), [d(TTAGGGp)]₄ (B), and [d(TTAGGGT)]₄ (C), respectively, in 300 mM KCl and 50 mM potassium phosphate buffer at pH6.80 and 25 °C. Plots of the 396 nm absorbance against concentrations of NG8I (A'), [d(TTAGGGp)]₄ (B'), and [d(TTAGGGT)]₄ (C'), respectively. The AcMP11 binding constant (K_a) values of $5.32 \pm 0.45 \mu\text{M}^{-1}$, $1.50 \pm 0.42 \mu\text{M}^{-1}$, and $0.14 \pm 0.01 \mu\text{M}^{-1}$ were obtained for the AcMP11–NG18I, AcMP11–[d(TTAGGGp)]₄, and AcMP11–[d(TTAGGGT)]₄ hybrid-complexes, respectively.

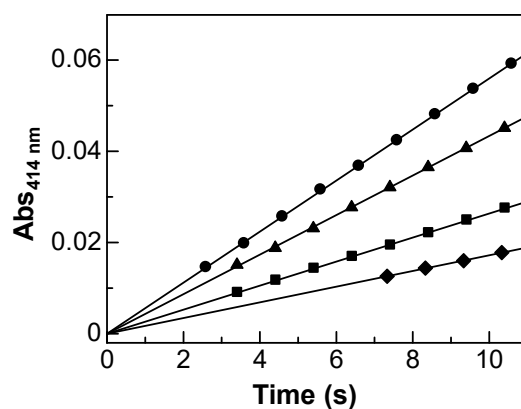


Fig. S11 Time-evolution of 414 nm absorbance due to ABTS oxidation by the AcMP11-[d(TTAGGG)]₄ (●), AcMP11-NG18I (▲), AcMP11-[d(TTAGGGp)]₄ (■), and AcMP11-[d(TTAGGGT)]₄ (◆) complexes. Samples comprised 0.1 μ M catalyst, 0.5 mM ABTS, and 4 mM H₂O₂ in 100 mM KCl and 50 mM potassium phosphate buffer, pH6.80 at 25 °C.

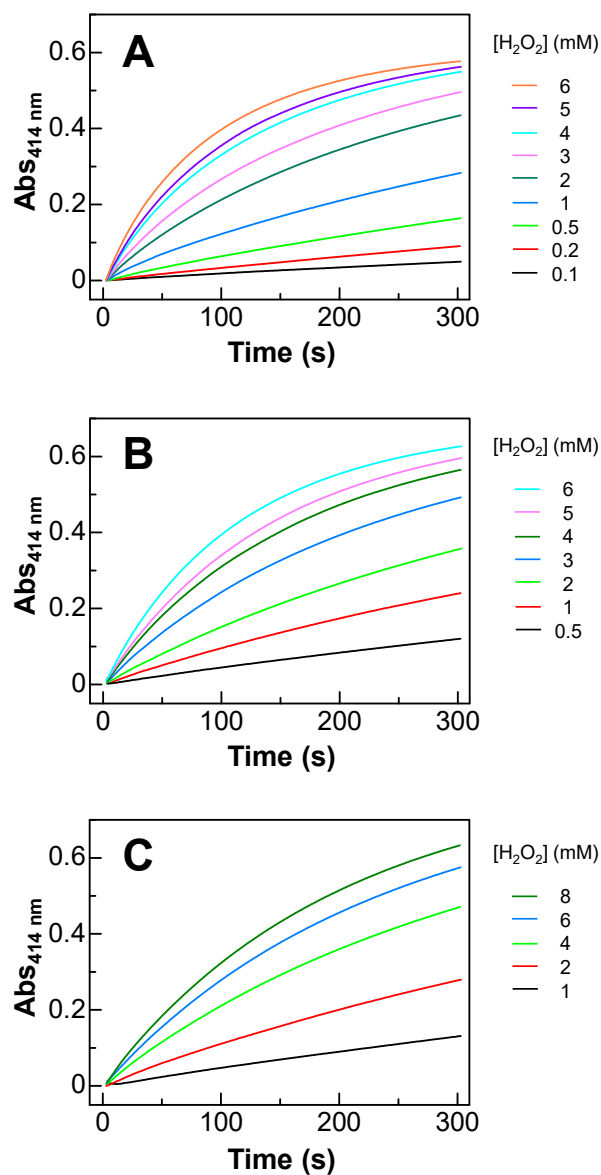


Fig. S12 Time-evolution of 414 nm absorbance due to ABTS oxidation by the (A) AcMP11-[d(TTAGGG)]₄, (B) AcMP11-NG18I, and (C) AcMP11-[d(TTAGGGp)]₄ hybrid-complexes. Samples comprised 0.1 μ M catalyst, 0.5 mM ABTS, and 0 – 8 mM H_2O_2 in 100 mM KCl and 50 mM potassium phosphate buffer, pH6.80 at 25 °C.